

Molybdenum Site Structure of MOSC Family Proteins

Logan J. Giles,[†] Christian Ruppelt,[‡] Jing Yang,[†] Ralf R. Mendel,^{*,‡} Florian Bittner,^{*,‡} and Martin L. Kirk^{*,†}[†]Department of Chemistry and Chemical Biology, The University of New Mexico, MSC03 2060, 1 University of New Mexico, Albuquerque, New Mexico 87131-0001, United States[‡]Department of Plant Biology, Braunschweig University of Technology, Humboldtstrasse 1, 38023 Braunschweig, Germany

Supporting Information

ABSTRACT: Mo K-edge X-ray absorption spectroscopy has been used to probe as-isolated structures of the MOSC family proteins pmARC-1 and HMCS-CT. The Mo K-edge near-edge spectrum of HMCS-CT is shifted ~ 2.5 eV to lower energy compared to the pmARC-1 spectrum, which indicates that as-isolated HMCS-CT is in a more reduced state than pmARC-1. Extended X-ray absorption fine structure analysis indicates significant structural differences between pmARC-1 and HMCS-CT, with the former being a dioxo site and the latter possessing only a single terminal oxo ligand. The number of terminal oxo donors is consistent with pmARC-1 being in the Mo^{VI} oxidation state and HMCS-CT in the Mo^{IV} state. These structures are in accord with oxygen-atom-transfer reactivity for pmARC-1 and persulfide bond cleavage chemistry for HMCS-CT.

Members of the molybdenum cofactor (Moco) sulfuryase C-terminal (MOSC) domain superfamily of pyranopterin molybdenum (Mo) proteins are known to play significant roles in Moco maturation, prodrug activation, detoxification of possible mutagens, and the regulation of intracellular nitric oxide (NO) levels.^{1–4} Moco sulfuryase proteins are essential for the activation of Mo enzymes of the xanthine oxidase family. In this activation process, the N-terminal domain of Moco sulfuryase decomposes free L-cysteine with concomitant release of sulfur, which is subsequently transferred to the Moco that is bound to the C-terminal domain of the protein.^{5,6} Once sulfuryated Moco is generated, the MOSC domain is capable of activating its target enzymes in a final maturation step. In addition to Moco sulfuryases, the MOSC superfamily in eukaryotes also comprises the mitochondrial amidoxime reducing component (mARC) proteins, which are located in the outer mitochondrial membrane and catalyze the Moco-dependent reduction of a diverse range of N-hydroxylated substrates that include amidoximes, N-hydroxysulfonamides, and N-hydroxyguanidines.^{4,7–12} Many of these substrates serve as prodrugs that are readily absorbed in the stomach and intestines and then are converted to their active forms by mARC enzymes. In spite of the role that mARC plays in prodrug activation, its exact biological function remains elusive. Yet, because of the known function of Moco sulfuryases, a general role of MOSC proteins in metal–sulfur cluster biogenesis has been discussed.¹³ Both mARC and Moco sulfuryase have been shown to be related based on their sequence similarity^{13,14} but

have yet to be characterized by X-ray crystallography. This fundamental gap in the knowledge base has hindered our ability to determine key structure/function relationships for MOSC family proteins. Here, we use a combination of X-ray absorption near-edge structure (XANES) and extended X-ray absorption fine structure (EXAFS) at the Mo K-edge to probe the coordination environment of plant mARC isoform 1 (pmARC-1) and the human Moco sulfuryase C-terminal domain (HMCS-CT).

The XANES spectra for as-isolated, aerobic pmARC-1 and HMCS-CT are presented in Figure 1. These spectra derive from

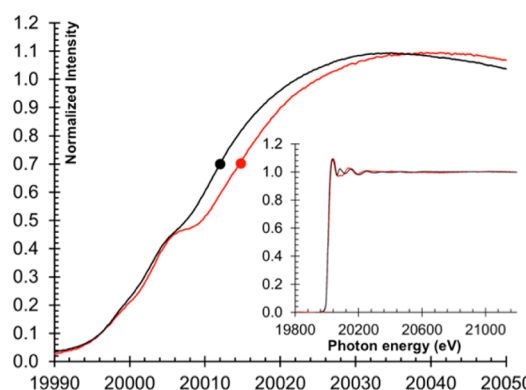


Figure 1. Mo K-edge XANES spectra of as-isolated HMCS-CT (black) and as-isolated pmARC-1 (red). Inset: Complete $k = 18$ spectra.

the promotion of a Mo 1s core electron to valence molecular orbitals and are therefore sensitive probes of the geometric and electronic structures of the Mo sites.¹⁵ The XANES spectrum of pmARC-1 is shifted ~ 2.5 eV to higher energy relative to that of HMCS-CT, which indicates that as-isolated pmARC-1 is more oxidized than HMCS-CT. The 1s \rightarrow Mo \equiv O transition is clearly observed at $\sim 20,006$ eV in the pmARC-1 spectrum, and its relative intensity is indicative of a greater number of terminal oxo ligands^{16–20} bound to the Mo ion in pmARC-1 compared to HMCS-CT. This observation, coupled with the ~ 2.5 eV edge shift, is consistent with the Mo ion of pmARC-1 being a dioxo Mo^{VI} site and HMCS-CT possessing a monooxo Mo^{IV} site.²¹

We have used EXAFS to determine the number of terminal oxo ligands and provide details regarding the nature of the first

Received: July 3, 2014

Published: August 28, 2014

coordination sphere. The pmARC-1 EXAFS and best fit to the data are presented in Figure 2. The best fit to the data reveals a

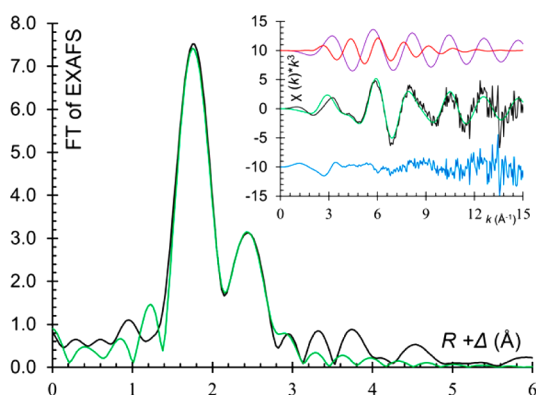


Figure 2. Mo EXAFS of pmARC-1 (black) and the corresponding FT of fit 1-1 (green). Inset: (top) Mo=O (red) and Mo-S (purple) scattering paths that contribute to the overall fit; (middle) k -space data for pmARC-1 (black) and fit 1-1 (green); (bottom) residual (blue).

single oxygen shell consisting of two terminal oxo ligands (mean $d_{\text{Mo=O}} = 1.76 \text{ \AA}$) and one sulfur shell comprised of three sulfur donors (mean $d_{\text{Mo-S}} = 2.47 \text{ \AA}$). Additional fits to the data are included in Table 1. The presence of two terminal oxo donors is consistent with the observation of the intense $1s \rightarrow \text{Mo}\equiv\text{O}$ transition that is observed in the pmARC-1 XANES spectrum. Analysis of the EXAFS data results in a proposed structure (Figure 4A) for pmARC-1 that is remarkably similar to oxidized sulfite oxidase (SO), with two terminal oxo ligands, a pyranopterin dithiolene, and a coordinated cysteine. Although the electron paramagnetic resonance spectra of pmARC and the “low-pH” forms of SO are similar,²⁸ pmARC-1 does not possess the SO (SUOX) fold,²² suggesting that the MOCS family proteins are distinct from the SO family enzymes. As such, there is no *a priori* evidence that suggests that mARC and the SO family enzymes possess similar active site geometries.

The HMCS-CT EXAFS (Figure 3) is markedly different from that of pmARC-1, as was anticipated from the differences observed in the XANES spectra. More specifically, the relative intensities of the oxo shell at 1.71 \AA and sulfur shell at 2.47 \AA are reversed with respect to the pmARC data, and this indicates that the ratio of oxo to sulfur ligands in HMCS-CT is different from that observed for pmARC-1. The best fit to the HMCS-CT

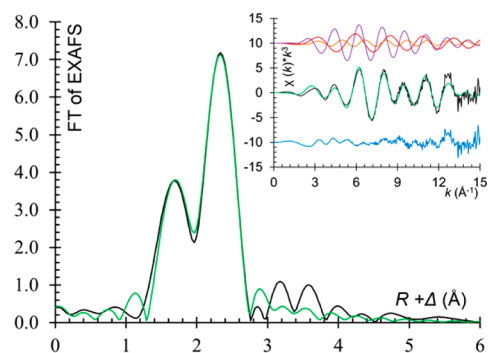


Figure 3. Mo EXAFS for HMCS-CT (black) and the corresponding FT of fit 2-1 (green). Inset: (top) Mo=O (red), Mo-O (orange), and Mo-S (purple) scattering paths that contribute to the overall fit; (middle) k -space data for HMCS-CT (black) and fit 2-1 (green); (bottom) residual (blue).

EXAFS is obtained with two oxygen shells consisting of a single terminal oxo ligand ($d_{\text{Mo=O}} = 1.70 \text{ \AA}$) and a longer Mo-O vector at 2.49 \AA , and a single sulfur shell comprised of three sulfur donors (mean $d_{\text{Mo-S}} = 2.47 \text{ \AA}$). Analysis of the HMCS-CT EXAFS data results in the proposed structure depicted in Figure 4B, where the Mo^{IV} ion is coordinated by a single terminal oxo, a

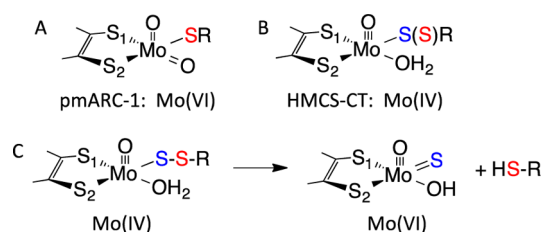


Figure 4. Possible structures for as-isolated pmARC-1 (A) and HMCS-CT (B) determined from XAS. (C) Internal redox conversion of the molybdenum(IV) persulfide to form a Mo^{VI}=S species and uncoordinated cysteine.

pyranopterin dithiolene, a cysteine or cysteine persulfide,^{2,6} and possibly a weakly bound aqua ligand or light atom donor (i.e., nitrogen, oxygen) from a protein-derived ligand. Attempts to model the data with a coordinated persulfide donor did not improve the quality of the fit. Thus, the coordination geometry of

Table 1. EXAFS Curve-Fitting Results for MOSC Proteins

	fit	Mo≡O			Mo-S			Mo-O			ΔE_0	R_F (%)
		N	R	σ^2	N	R	σ^2	N	R	σ^2		
pmARC-1	fit 1-1	2.0	1.76	0.002	3.0	2.47	0.013				-3.76	8.79
	fit 1-2	3.0	1.76	0.005	2.0	2.45	0.009				-5.48	15.79
	fit 1-3	3.0	1.76	0.005	3.0	2.45	0.013				-5.78	13.38
	fit 1-4	1.0	1.76	0.001 ^a	3.0	2.43	0.010	1.0	2.43	0.001 ^a	-6.94	33.98
	model 1-1 ^b	2	1.71		3	2.46						
HMCS-CT	fit 2-1	1.0	1.71	0.002	3.0	2.38	0.006	1.0	2.49	0.004	-8.97	5.51
	fit 2-2	1.0	1.71	0.002	3.0	2.37	0.006				-7.97	6.66
	fit 2-3	2.0	1.72	0.008	2.0	2.37	0.006				-7.24	12.09
	model 2-1 ^c	1	1.69		3	2.36		1	2.31			
	model 2-2 ^d	1	1.70		3	2.34						

^aThe σ^2 value was fixed to 0.001 to avoid negative σ^2 values. ^bGeometry-optimized model structure consistent with fit 1-1. ^cGeometry-optimized model structure consistent with fit 2-1. ^dGeometry-optimized model structure consistent with fit 2-2. Details on the model calculations are given in the Supporting Information.

as-isolated HMCS-CT appears to be similar to that of reduced SO family enzymes.

In summary, we have used Mo K-edge X-ray absorption spectroscopy (XAS) to illuminate differences in the coordination geometry of the MOSC family proteins pmARC-1 and HMCS-CT. The proposed structure of as-isolated pmARC-1 is consistent with a dioxo Mo^{VI} site similar to that found for oxidized enzymes of the SO family. While the exact biological function of the mARC proteins is not known, mARC proteins have been shown to function as oxygen-atom-transfer catalysts in the reduction of amidoxime prodrug substrates. Thus, the structure supports a proposed catalytic cycle with the Mo ion cycling between monooxo Mo^{IV} and dioxo Mo^{VI} oxidation states and an oxygen atom transferring from the substrate to the Mo center. Two sequential e⁻/H⁺ transfer steps regenerate the catalytically competent Mo^{IV} state. The XAS structure proposed for HMCT-CT is unique in that it is the only human pyranopterin molybdenum protein that is in the reduced monooxo Mo^{IV} state in its as-isolated form. The Mo^{IV} oxidation state is consistent with HMCS-CT accepting a sulfur atom from the HMCS N-terminal domain to form a Mo-bound cysteine persulfide. Persulfide coordination to Mo has been suggested for HMCS^{2,6} and periplasmic nitrate reductases.^{23–25} An induced internal electron transfer from Mo^{IV} to the Mo-bound cysteine persulfide would then result in cleavage of the persulfide bond and transfer of the sulfane (terminal) sulfur to the Mo as a bound sulfido ligand (Figure 4C) prior to transfer of the intact cofactor into apo XO. Such induced internal electron-transfer reactivity between Mo and persulfides was shown by Stiefel and co-workers over 30 years ago.^{26,27} Our initial calculations show that the molybdenum(IV) persulfide is a stable species but can convert to the Mo^{VI}=S form by protonation of the bridging persulfide sulfur with subsequent or concurrent deprotonation of the aqua ligand.

■ ASSOCIATED CONTENT

■ Supporting Information

Cloning, expression, and purification of pmARC and HMCS-CT, XAS experimental, Athena and Artemis data analysis and fitting information, and computational modeling details. This material is available free of charge via the Internet at <http://pubs.acs.org>.

■ AUTHOR INFORMATION

Corresponding Authors

*E-mail: r.mendel@tu-bs.de.

*E-mail: f.bittner@tu-bs.de.

*E-mail: mkirk@unm.edu.

Notes

The authors declare no competing financial interest.

■ ACKNOWLEDGMENTS

M.L.K. acknowledges the National Institutes of Health (NIH; Grant GM 057378) for financial support. F.B. acknowledges financial support from the Deutsche Forschungsgemeinschaft (Bi 1075/2-2). Use of the Stanford Synchrotron Radiation Lightsource, SLAC National Accelerator Laboratory, is supported by the U.S. Department of Energy (DOE), Office of Science, Office of Basic Energy Sciences, under Contract E-AC02-76SF00515. The SSRL Structural Molecular Biology Program is supported by the DOE Office of Biological and Environmental Research and by the NIH NIGMS (including

P41GM103393). The contents of this publication are solely the responsibility of the authors and do not necessarily represent the official views of NIGMS or NIH. We thank SSRL staff and scientists, especially Matthew Latimer, Erik Nelson, and Ritimukta Sarangi, for their support at BL 7-3.

■ REFERENCES

- (1) Sparacino-Watkins, C. E.; Tejero, J. S.; Sun, B.; Gauthier, M. C.; Thomas, J.; Ragireddy, V.; Merchant, B. A.; Wang, J.; Azarov, I.; Basu, P.; Gladwin, M. T. *J. Biol. Chem.* **2014**, *289*, 10345.
- (2) Hille, R.; Hall, J.; Basu, P. *Chem. Rev.* **2014**, *114*, 3963.
- (3) Havemeyer, A.; Lang, J. A.; Clement, B. *Drug Metab. Rev.* **2011**, *43*, 524.
- (4) Kotthaus, J.; Wahl, B.; Havemeyer, A.; Kotthaus, J.; Schade, D.; Garbe-Schönberg, D.; Mendel, R.; Bittner, F.; Clement, B. *Biochem. J.* **2011**, *433*, 383.
- (5) Lehrke, M.; Rump, S.; Heidenreich, T.; Wissing, J.; Mendel, R. R.; Bittner, F. *Biochem. J.* **2012**, *441*, 823.
- (6) Wollers, S.; Heidenreich, T.; Zarepour, M.; Zachmann, D.; Kraft, C.; Zhao, Y. D.; Mendel, R. R.; Bittner, F. *J. Biol. Chem.* **2008**, *283*, 9642.
- (7) Havemeyer, A.; Grünwald, S.; Wahl, B.; Bittner, F.; Mende, R.; Erdélyi, P.; Fischer, J.; Clement, B. *Drug Metab. Dispos.* **2010**, *38*, 1917.
- (8) Gruenewald, S.; Wahl, B.; Bittner, F.; Hungeling, H.; Kanzow, S.; Kotthaus, J.; Schwering, U.; Mendel, R. R.; Clement, B. *J. Med. Chem.* **2008**, *51*, 8173.
- (9) Havemeyer, A.; Bittner, F.; Wollers, S.; Mendel, R.; Kunze, T.; Clement, B. *J. Biol. Chem.* **2006**, *281*, 34796.
- (10) Andersson, S.; Hofmann, Y.; Nordling, A.; Li, X.-q.; Nivelius, S.; Andersson, T. B.; Ingelman-Sundberg, M.; Johansson, I. *Drug Metab. Dispos.* **2005**, *33*, 570.
- (11) Clement, B.; Behrens, D.; Amschler, J.; Matschke, K.; Wolf, S.; Havemeyer, A. *Life Sci.* **2005**, *77*, 205.
- (12) Clement, B.; Mau, S.; Deters, S.; Havemeyer, A. *Drug Metab. Dispos.* **2005**, *33*, 1740.
- (13) Anantharaman, V.; Aravind, L. *FEMS Microbiol. Lett.* **2002**, *207*, 55.
- (14) Hille, R.; Nishino, T.; Bittner, F. *Coord. Chem. Rev.* **2011**, *255*, 1179.
- (15) Pushie, M. J.; George, G. N. *Coord. Chem. Rev.* **2011**, *255*, 1055.
- (16) Joyner, R. W.; Martin, K. J.; Meehan, P. J. *Phys. C: Solid State Phys.* **1987**, *20*, 4005.
- (17) Cramer, S.; Wahl, R.; Rajagopalan, K. *J. Am. Chem. Soc.* **1981**, *103*, 7721.
- (18) Kutzler, F. W.; Scott, R. A.; Berg, J. M.; Hodgson, K. O.; Doniach, S.; Cramer, S. P.; Chang, C. H. *J. Am. Chem. Soc.* **1981**, *103*, 6083.
- (19) George, G. N.; Garrett, R. M.; Prince, R. C.; Rajagopalan, K. V. *J. Am. Chem. Soc.* **1996**, *118*, 8588.
- (20) Pushie, M. J.; Doonan, C. J.; Moquin, K.; Weiner, J. H.; Rothery, R.; George, G. N. *Inorg. Chem.* **2011**, *50*, 732.
- (21) George, G. N.; Kipke, C. A.; Prince, R. C.; Sunde, R. A.; Enemark, J. H.; Cramer, S. P. *Biochemistry* **1989**, *28*, 5075.
- (22) Workun, G. J.; Moquin, K.; Rothery, R. A.; Weiner, J. H. *Microbiol. Mol. Biol. Rev.* **2008**, *72*, 228.
- (23) Najmudin, S.; Gonzalez, P. J.; Trincao, J.; Coelho, C.; Mukhopadhyay, A.; Cerqueira, N.; Romao, C. C.; Moura, I.; Moura, J. J. G.; Brondino, C. D.; Romao, M. J. *J. Biol. Inorg. Chem.* **2008**, *13*, 737.
- (24) Coelho, C.; Gonzalez, P. J.; Trincao, J.; Carvalho, A. L.; Najmudin, S.; Hettman, T.; Dieckman, S.; Moura, J. J. G.; Moura, I.; Romao, M. J. *Acta Crystallogr., Sect. F: Struct. Biol. Cryst. Commun.* **2007**, *63*, 516.
- (25) Sparacino-Watkins, C.; Stolz, J. F.; Basu, P. *Chem. Soc. Rev.* **2014**, *43*, 676.
- (26) Pan, W.-h.; Harmer, M. A.; Halbert, T. R.; Stiefel, E. I. *J. Am. Chem. Soc.* **1984**, *106*, 459.
- (27) Burgmayer, S. J. N.; Stiefel, E. I. *J. Chem. Educ.* **1985**, *62*, 943.
- (28) Wahl, F.; Reichmann, D.; Nkks, D.; Krompholz, N.; Havemeyer, A.; Clement, B.; Messerschmidt, T.; Rothkegel, M.; Biester, H.; Hille, R.; Mendel, R. R.; Bittner, F. *J. Biol. Chem.* **2010**, *285*, 37847.